Interplay between thermoelectric and structural properties of type-I clathrate $K_8Ga_8Sn_{38}$ single crystals

T. Tanaka,[1] T. Onimaru,[1,*] K. Suekuni,[1] S. Mano,[1] H. Fukuoka,[2] S. Yamanaka,[2] and T. Takabatake[1,3]
[1]*Department of Quantum Matter, ADSM, Hiroshima University, Higashi-Hiroshima 739-8530, Japan*
[2]*Department of Applied Chemistry, Graduate School of Engineering, Hiroshima University, Higashi-Hiroshima 739-8527, Japan*
[3]*Institute for Advanced Materials Research, Hiroshima University, Higashi-Hiroshima 739-8530, Japan*
(Received 8 February 2010; revised manuscript received 28 March 2010; published 19 April 2010)

We report structural, transport, and thermal properties of type-I clathrate $K_8Ga_8Sn_{38}$ single crystals grown by the self-flux method. Single-crystal x-ray diffraction analysis confirmed that the guest K^+ ion locates on the center in the tetrakaidecahedron composed of Ga and Sn atoms. The thermopower is largely negative, $-200\ \mu V/K$ at room temperature, irrespective of the flux used during growth (Ga or Sn). The thermal conductivity $\kappa(T)$ exhibits a large peak at 14 K. These observations in $K_8Ga_8Sn_{38}$ are contrasting with the splitting of the guest site and the glasslike behavior in $\kappa(T)$ reported for type-I $Ba_8Ga_{16}Sn_{30}$ although the free space for the guest is almost the same in both compounds. The electrostatic potential for the tetrakaidecahedron was calculated using the occupation probabilities of Ga ions in the three sites on the cage. It is found that the off-centered state is stabilized for the Ba^{2+} ions in $Ba_8Ga_{16}Sn_{30}$ by the partial occupation of Ga anion in the 16*i* site while the on-center state for $K_8Ga_8Sn_{38}$ is stabilized by the strongly preferred occupation of Ga anions in the 6*c* site. We conclude that the charge distribution on the cage is crucial for the splitting of the guest site into off-center positions in the tetrakaidecahedron of the type-I clathrate.

DOI: 10.1103/PhysRevB.81.165110 PACS number(s): 72.15.Jf, 72.20.Pa, 82.75.−z

I. INTRODUCTION

Thermoelectric materials have attracted much attention over the decades because of their potential for directly converting waste heat to electricity.[1] In searching for novel thermoelectric materials, Slack proposed the concept "phonon glass electron crystal (PGEC)."[2] The ideal PGEC material would have thermal properties similar to those of amorphous materials where phonons have short mean-free path and electronic properties similar to those of covalent crystals where electrons have high mobility. The thermoelectric efficiency of a given material is evaluated by the dimensionless figure of merit $ZT=S^2T/\rho\kappa$, with thermopower S, electrical resistivity ρ, and thermal conductivity κ. Among type-I clathrates with the general formula $A_8E_xX_{46-x}$, Ge-based compounds $A_8Ga_{16}Ge_{30}$ $(A=\mathrm{Ba,Sr})$ demonstrated unusually low $\kappa(1-2\ \mathrm{W/K\,m})$, rather low ρ $(\sim 1\ \mathrm{m\Omega\,cm})$, and large $S(-50\ \mu\mathrm{V/K})$ at 300 K.[3–5] Therefore, they were considered as materials satisfying the concept of PGEC. As is shown in Fig. 1(a), type-I crystal structure consists of two types of cages—dodecahedra and tetrakaidecahedra—both of which encapsulate A atoms as guests. The guest is bonded loosely to the cage framework which is made of sp^3-like covalent bonding of Ga and Ge atoms. The guest atoms vibrate with large amplitude in oversized cages, whose modes can resonantly scatter the acoustic phonons that carry most of the heat in the crystal. So far, clathrates with divalent guests such as $A_8Ga_{16}Ge_{30}$ $(A=\mathrm{Ba,Sr,Eu})$ have been extensively studied.[6–8] On going from $A=$Ba to $A=$Sr, and Eu in this series, the ionic radius decreases and the smallest Eu atoms in the tetrakaidecahedron occupy the split 24*k* sites, which are about 0.4 Å away from center.[9] Concomitantly, the vibration energy of the guest is lowered from 60 K to 53 K and 30 K.[6,10,11] As a result, the lattice thermal conductivity κ_L is suppressed more strongly. Furthermore, $\kappa_L(T)$ for $A=$Sr and Eu shows glasslike behavior with a plateau in the temperature range 10–20 K. It was proposed that the rattling motion of Eu ions among split sites in tetrakaidecahedron is responsible for the strong scattering of acoustic phonons.[6,12]

Another type-I clathrate $Ba_8Ga_{16}Sn_{30}$ (BGS) has a lattice parameter of 11.685 Å which is larger than that for $Ba_8Ga_{16}Ge_{30}$ (BGG).[13] As a consequence of the large guest free space for the Ba atoms in the tetrakaidecahedron of BGS, the Ba atoms occupy off-center 24*k* sites which are 0.4 Å away from center 6*d* site.[13,14] The κ_L of BGS is the lowest among intermetallic type-I clathrates at 4 K. It shows glasslike temperature dependence and approaches 0.75 W/K m on heating to 150 K. The characteristic energy for the rattling motion of Ba atoms in tetrakaidecahedron is approximately 20 K.[14,15] Therefore, BGS was proved to be a typical material which satisfies the concept of PGEC. Furthermore, it was naturally conjectured that the large free space of the guest is necessary for stabilizing the split sites.[15] As for thermoelectric material, BGS has an advantage that the carrier type in the samples can be tuned by choosing the

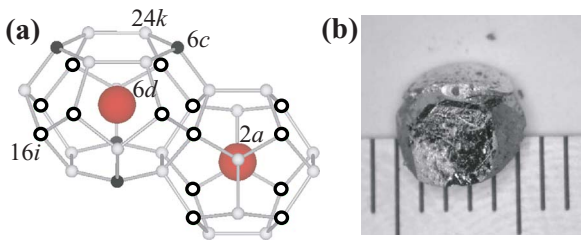

FIG. 1. (Color online) (a) Type-I clathrate structure composed of tetrakaidecahedron and dodecahedron with guest atoms at 6*d* and 2*a* sites, respectively. The tetrakaidecahedron is composed of cage atoms at 6*c*, 16*i*, and 24*k* sites, which are shown by black, white and dark spheres, respectively. (b) Photograph of $K_8Ga_8Sn_{38}$ single crystal grown from Ga flux.

self-flux. Namely, with Ga flux, holes are doped in the system and thus S is largely positive, 300 μV/K at 290 K. With Sn flux, on the other hand, electrons are doped and S is largely negative, −300 μV/K at 290 K.[15]

Type-I Sn-based clathrates encapsulating alkaline metals K, Rb, and Cs in the cage are also known to exist. There are reports on $K_8Ga_8Sn_{38}$ (KGS), $Rb_8Ga_8Sn_{38}$, $Cs_8Ga_8Sn_{38}$, and $K_8Al_8Sn_{38}$.[13,16–18] The chemical composition of 8:8:38 satisfies the Zintl rule, whereby one electronic charge is transferred from the alkaline metal cation to Ga on the cage to form sp^3-like covalently bonded framework. In fact, semiconducting behavior was reported for $Rb_8Ga_8Sn_{38}$.[19] In order to further understand the unusual structural and thermal properties of BGS as mentioned above, we have focused our attention to KGS whose lattice parameter of 11.935 Å and guest ionic radius for K in a high coordination environment of 1.64 Å (Ref. 20) are close to those of BGS (11.685 Å and 1.61 Å), respectively. The previous study of single-crystal x-ray diffraction of KGS found that the K atom at 6d site in the tetrakaidecahedron vibrates with unusually large amplitude in the middle plane parallel to the hexagonal rings.[17] In fact, the atomic displacement parameters (ADPs), $U_{22}=U_{33}=0.12$ Å^2 are five times larger than those for the K atom at 2a site in the dodecahedron. The thermoelectric properties of KGS at temperatures between 300 and 520 K have been reported on polycrystalline samples prepared by the spark plasma sintering method.[21] While the κ_L of 1.1 W/K m at 300 K is larger than that for BGS, the high mobility of 25 cm^2/V s and largely negative S of −250 μV/K are promising results for thermoelectric application. The maximum ZT value of 0.27 was estimated at 490 K.[21]

II. SINGLE-CRYSTAL GROWTH AND STRUCTURAL ANALYSIS

We have grown single crystals of KGS by self-flux method using both Sn and Ga as flux. Two kinds of elemental mixtures with the atomic ratios of 8:8:60 and 8:15:38 for K:Ga:Sn were used. The samples from these batches will be referred as Sn#1 and Ga#2, respectively. High-purity elements K, Ga, and Sn were put into a molybdenum crucible, which was in turn sealed in a stainless-steel ampoule. All manipulations were performed inside a glove box under an argon atmosphere with water concentration less than 0.06 ppm. The Sn#1 sample was heated up to 900 °C, kept at 700 °C for 1 week, then cooled at a rate of 1 °C/h to 450 °C. At this point, the ampoule was quickly removed from the furnace and the remaining molten Sn flux was separated by centrifuging. On the other hand, the Ga#2 sample was heated up to 550 °C, then cooled at a rate of 1 °C/h to 450 °C.

The obtained crystals are 3.5–5.0 mm in diameter, as shown in Fig. 1(b). Powder x-ray diffraction patterns with Cu Kα radiation were recorded using a Rigaku Ultima IV diffractometer. The patterns were in good agreement with those simulated with reported atomic coordinates,[17] and the Rietveld analysis led to the lattice parameter of 11.964 Å for both samples. The crystal composition was determined by electron probe microanalysis (EPMA) using JEOL JXA-8200 analyzer. The crystal composition and starting composition are listed in Table I, where the composition of K was assumed to be 8. We find that the crystal composition does not depend on the starting composition and is nearly stoichiometric. In order to determine the melting point, the differential thermal analysis (DTA) was done using SETARAM DTA-92–18. The DTA curve recorded on heating at a rate of 5 °C/min exhibited an endothermic peak at 600 °C. The fall-off point at 580 °C was taken as the melting point.

TABLE I. Starting composition, crystal composition, and lattice parameter of $K_8Ga_8Sn_{38}$ samples at 300 K.

	Starting composition			Crystal composition			Lattice parameter
Sample	K	Ga	Sn	K	Ga	Sn	a (Å)
Sn#1	8	8	60	8.0	7.8(2)	37.9(2)	11.964(4)
Ga#2	8	15	38	8.0	7.9(2)	37.9(2)	11.964(9)

Single-crystal x-ray diffraction measurements were performed on selected crystals of 0.1 mm in diameter. We used a Rigaku RAPID-S diffractometer with an imaging plate area detector using monochromatic Mo Kα radiation (λ =0.71073 Å). The data were recorded at various constant temperatures from 120 to 290 K. The crystal structure was refined using the Rigaku CRYSTALSTRUCTURE crystallographic software package.[22] We confirmed the cubic symmetry with the space group $Pm\bar{3}n$ (No. 223). The lattice parameter of a=11.967(1) Å is in good agreement with the value of 11.964 Å obtained by powder x-ray diffraction analysis. The final value of the reliability factor $R(R_W)$ is 0.0098 (0.0119). Such low values for a complex and disordered system evidence the good crystallinity of the sample and the validity of the structural model. The refined atomic coordinates, isotropic displacement parameters U_{eq}, and occupational parameters at room temperature are summarized in Table II, where K(1) and K(2) are guests in dodecahedron and tetrakaidecahedron, respectively.

In order to examine the possible occupation of K(2) on off-center 24k site, we treated the atomic coordinates of K(2) as free parameters. Even though the K(2) atoms were initially placed at off-center sites, the coordinates after iteration have converged on (1/4, 1/2, 0) which is the center 6d site. This result contrasts markedly with the occupation of off-center 24k site for Ba(2) ions in BGS despite having similar free space for the guest as for K(2) ions in KGS. Note that the isotropic displacement parameter U_{eq} of K(2) is several times larger than that of K(1). Moreover, anisotropic displacement parameter U_{22} and U_{33} of K(2) in the middle plane parallel to the hexagonal rings of tetrakaidecahedron are unusually large as 0.1040(14) Å^2 compared to U_{11} =0.0432(15) Å^2 for the out of the plane motion. The occupational parameters of cage atoms listed in Table II indicate that Sn atoms occupy 16i and 24k sites preferentially while Ga atoms preferentially occupy 6c site. Because the distance between 6c site and nearest-neighbor 24k site is shortest among all cage bond distances, Ga has a greater tendency to occupy 6c site so that the Ga-Ga bonding with higher bond-

TABLE II. Atomic coordinates, isotropic displacement parameters U_{eq}, and occupational parameters at 300 K, obtained from structural refinement of a $K_8Ga_8Sn_{38}$ single crystal.

Atom	Site	x	y	z	U_{eq}(Å^2)	Occupancy
K(1)	2a	0	0	0	0.0299(3)	1
K(2)	6d	1/4	1/2	0	0.0837(7)	1
Ga(1)/Sn(1)	6c	1/4	0	1/2	0.0186(2)	0.468(5)/0.530(5)
Ga(2)/Sn(2)	16i	0.18316(1)	0.18316(1)	0.18316(1)	0.0160(1)	0.086(2)/0.914(2)
Ga(3)/Sn(3)	24k	0	0.31270(2)	0.11864(2)	0.0165(1)	0.158(2)/0.842(2)

ing energy than others is avoided, as was reported for BGG and BGS.[15,23,24]

The x-ray diffraction data at various temperatures were refined to obtain the ADP for K and Ga/Sn. Figure 2 represents the temperature variations in ADP and the inset shows that of the lattice parameter. Assuming the guest K atom as an Einstein oscillator and the cage as a Debye solid, the parameters U_{11} and U_{22} for the guest K atom and U_{eq} for the framework Ga/Sn atoms at a given temperature T are respectively written as

$$U_{ii}(\mathrm{K}) = \frac{\hbar^2}{2m_g k_B \theta_{E_{ii}}} \coth\left(\frac{\theta_{E_{ii}}}{2T}\right) + d_{ii}^2 \qquad (i = 1,2), \quad (1)$$

$$U_{eq}(\mathrm{Ga/Sn}) = \frac{3\hbar^2 T}{m_{av} k_B \theta_D^2}\left[\frac{T}{\theta_D}\int_0^{\theta_D/T} \frac{x}{\exp(x)-1}dx + \frac{\theta_D}{4T}\right] + d^2, \quad (2)$$

where m_g, m_{av}, and d are mass of the guest atom K, the average mass of the framework atoms Ga/Sn, and temperature-independent disorder term, respectively.[25] As is shown in Fig. 2, the experimental ADPs are well fitted by using the above equations. Einstein temperatures derived from the fits to U_{eq} are 112 K and 72 K for K(1) and K(2), respectively. Considering the anisotropic vibration of K(2), we estimated Einstein temperatures of 97 K and 65 K from the fits to U_{11} and U_{22}, respectively. The Debye temperatures of cage atoms at the three sites are in the range between 174 and 175 K, which is lower than the values of 194–203 K reported for BGS.[15]

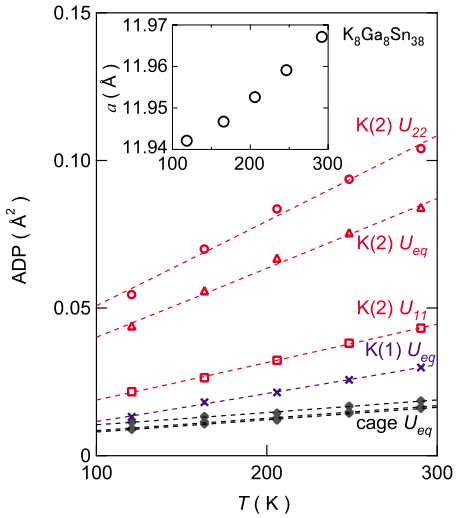

FIG. 2. (Color online) Temperature dependence of ADPs U_{eq} for K(1), U_{eq}, U_{11} and U_{22} for K(2) and U_{eq} for cage atoms for $K_8Ga_8Sn_{38}$. The dotted lines are the fits to the data using Eqs. (1) and (2) (see text). The inset shows the temperature dependence of lattice parameter.

III. TRANSPORT AND THERMAL MEASUREMENTS

The temperature-dependent electrical resistivity ρ and thermopower S were measured in the range from 4 to 300 K with homemade systems by a standard dc four-probe method and a differential method, respectively. In the latter, a temperature difference of 0.04–0.3 K was applied along a bar-shaped sample. In order to estimate the carrier density and mobility, the Hall coefficient R_H was measured by a dc method in a field of 1 T applied by a conventional electromagnet. The thermal conductivity κ was measured using a steady-state method in a range from 4 to 300 K. Because the effect of heat losses by radiation becomes serious in the measurement of κ at high temperatures, the lattice thermal conductivity was assumed to be constant above 150 K. The electronic contribution to κ was estimated from the measured $\rho(T)$ by using the Wiedemann-Franz law. Specific heat C was measured from 2 to 300 K on a Quantum Design physical property measurement system using its standard thermal-relaxation method. Figure 3 displays the sets of data of $\rho(T)$, $S(T)$, and $\kappa(T)$ for Sn#1 and Ga#2 samples. With increasing temperature, $\rho(T)$ monotonically increases and $S(T)$ linearly decreases for both samples. The negative sign of S for Ga#2 is opposite to our initial expectation that the Ga flux method would lead to excess Ga in the crystal and thus provide hole carriers, as in the case of BGS crystals grown from Ga flux.[15] If we assume one type carrier, the Hall coefficient $R_H = -0.20$ cm^3/C is translated to the electron charge-carrier density of 3.2×10^{19}/cm^3 at 290 K. This density equals to that reported for n-type BGS, while the value of $\rho(T=290\ \mathrm{K})$ is one fourth of that for n-type BGS. It suggests the higher mobility of carriers in KGS than in BGS. In fact, the Hall mobility estimated from R_H/ρ is 19 cm^2/V s for KGS, being four times larger than that for BGS. As was pointed out by Hayashi *et al.*,[21] the higher mobility may be a result of the higher ratio of Sn atoms among 46 atoms on the cage; 38/46 in KGS and 30/46 in BGS. This should result in more homogeneous sp^3 bonding in KGS than in BGS. As a consequence, the power factor S^2/ρ for KGS is as large as 0.65 mW/K^2 m at 290 K.

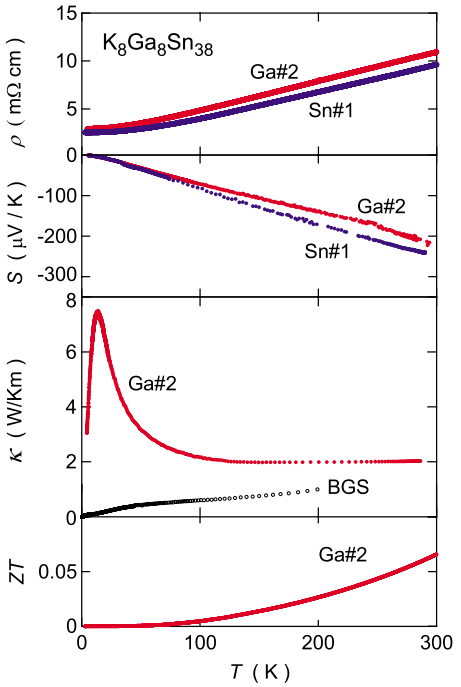

FIG. 3. (Color online) Temperature dependence of electrical resistivity ρ, thermopower S, thermal conductivity κ, and dimensionless figure of merit ZT for $K_8Ga_8Sn_{38}$. The data of $\kappa(T)$ for $Ba_8Ga_{16}Sn_{30}$ are taken from Ref. 15.

Figure 3 also displays $\kappa(T)$ for Ga#2 KGS together with that for n-type BGS. The $\kappa(T)$ for KGS has a peak of 7.3 W/K m at 14 K, which is a characteristic behavior of a crystalline solid.[26] This is a good contrast with the glasslike behavior for BGS in which the off-center rattling of Ba guest in the tetrakaidecahedron scatters the acoustic phonons effectively.[15] In this context, we note that the crystalline behavior of $\kappa(T)$ for KGS is consistent with the on-center vibration in the tetrakaidecahedron. At the bottom of Fig. 3, we plot the dimensionless figure of merit $ZT=S^2T/\rho\kappa$ for Ga#2 sample. The ZT approaches 0.07 at 300 K, not high enough for real application at around room temperature. Evaluation of ZT at higher temperatures is necessary to assess the optimal efficiency range.

The specific heat $C(T)$ provides important information on the guest vibrations in caged compounds.[7,27] The data of $C(T)$ for KGS are plotted as C/T^3 vs T in Fig. 4. There are contributions from Einstein modes of K(1) and K(2), Debye specific heat of the 46 cage atoms and charge carriers. The number of Debye modes was taken as $138(3\times46)$ per formula unit. In order to reduce the number of parameters for fitting, we assumed that the Einstein temperature for the isotropic vibration of K(1) equals that for the vibration of K(2) perpendicular to the cage's two hexagons. The Einstein temperature is denoted by θ_{E1}, and the other one describing in-plane vibration of K(2) is denoted by θ_{E2}. Thus, the number of Einstein modes with θ_{E1} is $12(1\times6+3\times2)$ and that with θ_{E2} is $12(2\times6)$ per formula unit.[27] This assumption is allowed by the fact that U_{11} for K(1) is comparable with U_{11} for K(2) as found by the structural refinement. The Debye temperature θ_D was estimated to be 201 K from the measurements of sound velocities.[28] From the C/T vs T^2 plot, the

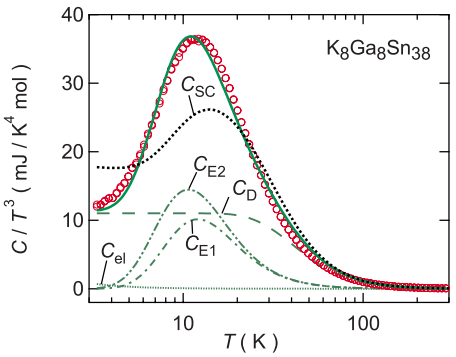

FIG. 4. (Color online) Temperature dependence of specific heat presented as C/T^3 vs T for $K_8Ga_8Sn_{38}$ (open circles). The solid line is the sum of Einstein contributions C_{E1} and C_{E2} with $\theta_{E1}=59.3$ K (dashed-dotted line) and $\theta_{E2}=51.2$ K (dashed double-dotted line), respectively, Debye contribution C_D with $\theta_D=201$ K (dashed line) and electronic contribution C_{el} with $\gamma=3.2$ mJ/K^2 mol (long dotted line). The dotted line (C_{SC}) represents the calculation using the Einstein and Debye temperatures obtained by single-crystal x-ray diffraction analysis (see text).

electronic specific-heat coefficient γ was estimated to be 3.2 mJ/K^2 mol, which is comparable with the value of 5.3 mJ/K^2 mol derived from the free-electron model for the carrier density of $n=3.2\times10^{19}/\mathrm{cm}^3$. Now, the residual parameters to fit the data of C/T^3 are only θ_{E1} and θ_{E2}, which were obtained as 59.3 K and 51.2 K, respectively. The fit is shown by the solid line in Fig. 4. The dotted line marked by C_{SC} represents the calculation using the parameters obtained from the analysis of the ADPs. Thereby, we used Einstein temperatures 112 K for K(1), 97 and 65 K for K(2), Debye temperature 175 K, and $\gamma=5.3$ mJ/K^2 mol estimated from the carrier density. This calculation gives a worse fit to the data compared to the fit described above. The possible reason is that the analysis of ADP's underestimated the Debye temperature because the range of the ADPs measurements up to 300 K is not sufficiently high compared with the Debye temperature.

IV. ANALYSIS OF ELECTROSTATIC POTENTIAL

The structural analysis showed that the K guest in KGS occupies the on-center 6d site in the tetrakaidecahedron. However, the Ba guest in BGS occupies the split sites despite having almost the same free space. It is important to understand the mechanism which stabilizes the split sites for the guest atom in the tetrakaidecahedron of type-I clathrate. The guest cation should feel the electrostatic potential created by cage anions. To calculate the potential, we assumed that Sn is electrically neutral and Ga has a point charge of $-e$. The Ga atoms in KGS occupy three sites, 6c, 16i, and 24k, as shown in Fig. 1(a), with occupation probabilities p_i given in Table I. The values of p_i in BGS are 0.707, 0.356, and 0.252 for 6c, 16i, and 24k sites, respectively.[15] Then, the electrostatic potential can be described as

$$\phi(\boldsymbol{r}) = \sum_i \frac{1}{4\pi\epsilon_0}\frac{-p_i e}{|\boldsymbol{r}_i - \boldsymbol{r}|}, \tag{3}$$

where $\boldsymbol{r}_i'$s are the coordinates of the Ga atoms. The calculated potentials in the middle plane between the two hexa-

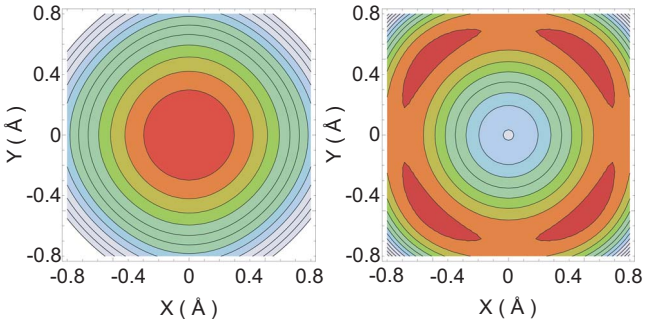

FIG. 5. (Color online) Electrostatic potential on the middle plane of the tetrakaidecahedron of the type-I clathrate calculated by assuming the Ga ion has a negative charge of $-e$. X and Y are coordinates with respect to the origin at 6d site. The potential minimum of K guest for $K_8Ga_8Sn_{38}$ is on-center (left) whereas that of Ba guest for $Ba_8Ga_{16}Sn_{30}$ is off-center (right).

gons in the tetrakaidecahedron are shown in Fig. 5 for KGS and BGS. The center is the 6d site and X denotes the local-symmetry axis along one of the three [100] directions. The potential minimum is on-center for KGS, whereas it is split into four positions which are 0.7 Å away from the center. It should be noted that the potential minimum is located on the 24j site rather than the 24k site as observed from single-crystal x-ray diffraction.[15] We calculated the potential by varying the values of p_i for the three sites and found that the splitting is made possible by the high probability of the occupancy of Ga anions on the 16i sites in BGS. In order to confirm this conjecture, we also calculated the potential for BGG with the value of p_i=0.74, 0.17, and 0.37 for 6c, 16i, and 24k sites, respectively.[23] The potential minimum is found to be on-center, which is consistent with the on-center vibration of Ba cations in BGG.[6] In Fig. 6, the arrangement of 16i and 24j sites is represented to understand better the relation between the preferential occupation of Ga anions on 16i site and the position of potential minimum. Our calculation indicates that the potential minimum shifts from 6d site to 24j site as p_i for the 16i site increases from 0.17 for BGG to 0.356 for BGS.

V. SUMMARY

We have reported structural and thermoelectric properties of single crystals of type-I clathrate KGS grown by self-flux method. On heating from 4 to 300 K, the thermopower linearly decreases to −200 μV/K and electrical resistivity monotonically increases from 3 to 10 mΩ cm. These behaviors do not depend on which flux Sn or Ga was used for the crystal growth. The thermal conductivity exhibits a peak of 7.3 W/K m at 14 K. This is a good contrast with the glass-like behavior of thermal conductivity in BGS for which rattling of Ba cations among four split sites in the tetrakaidecahedron is thought to be responsible. The on-center vibration of K cations in KGS was confirmed by single-crystal x-ray diffraction analysis. The calculation of electrostatic potential of the tetrakaidecahedron in BGS and KGS indicated that the preferential occupation of Ga ions with a negative charge plays the crucial role in determining whether or not the split sites are stabilized.

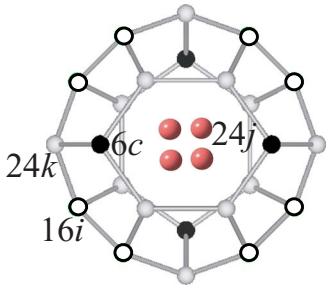

FIG. 6. (Color online) Side view of the tetrakaidecahedron to show the relation between the 16i site of the cage atom and the off-center 24j site for the guest atom.

ACKNOWLEDGMENTS

We would like to thank M. A. Avila for his critical reading of this manuscript and for guidance to the single-crystal growth by the flux method. We thank Y. Shibata for the EPMA performed at Natural Science Center for Basic Research and Development, Hiroshima University. This work was supported by a NEDO Grant No. 09002139-0 and Grant-in-Aid for Scientific Research from MEXT of Japan, Grants No. 1824032, No. 19051011, No. 21102516, and No. 20102004.

*onimaru@hiroshima-u.ac.jp

[1] For a recent review, see *Thermoelectrics Handbook Macro to Nano*, edited by D. M. Rowe (Taylor & Francis, Boca Raton, 2006).

[2] G. A. Slack, in *CRC Handbook of Thermoelectrics*, edited by D. M. Rowe (CRC, Boca Raton, FL, 1995), p. 407.

[3] J. L. Cohn, G. S. Nolas, V. Fessatidis, T. H. Metcalf, and G. A. Slack, Phys. Rev. Lett. **82**, 779 (1999).

[4] G. S. Nolas, J. L. Cohn, G. A. Slack, and S. B. Schujman, Appl. Phys. Lett. **73**, 178 (1998).

[5] A. Saramat, G. Svensson, A. E. C. Palmqvist, C. Stiewe, E. Mueller, D. Platzek, S. G. K. Williams, D. M. Rowe, J. D. Bryan, and G. D. Stucky, J. Appl. Phys. **99**, 023708 (2006).

[6] B. C. Sales, B. C. Chakoumakos, R. Jin, J. R. Thompson, and D. Mandrus, Phys. Rev. B **63**, 245113 (2001).

[7] S. Paschen, W. Carrillo-Cabrera, A. Bentien, V. H. Tran, M. Baenitz, Yu. Grin, and F. Steglich, Phys. Rev. B **64**, 214404 (2001).

[8] A. Bentien, M. Christensen, J. D. Bryan, A. Sanchez, S. Paschen, F. Steglich, G. D. Stucky, and B. B. Iversen, Phys. Rev. B **69**,

045107 (2004).
[9] B. C. Chakoumakos, B. C. Sales, and D. G. Mandrus, J. Alloys Compd. **322**, 127 (2001).
[10] Y. Takasu, T. Hasegawa, N. Ogita, M. Udagawa, M. A. Avila, K. Suekuni, I. Ishii, T. Suzuki, and T. Takabatake, Phys. Rev. B **74**, 174303 (2006).
[11] A. Bentien, V. Pacheco, S. Paschen, Yu. Grin, and F. Steglich, Phys. Rev. B **71**, 165206 (2005).
[12] R. Baumbach, F. Bridges, L. Downward, D. Cao, P. Chesler, and B. C. Sales, Phys. Rev. B **71**, 024202 (2005).
[13] H. G. von Schnering, R. Kröner, H. Menke, K. Peters, and R. Nesper, Z. Kristallogr. - New Cryst. Struct. **213**, 679 (1998).
[14] M. A. Avila, K. Suekuni, K. Umeo, H. Fukuoka, S. Yamanaka, and T. Takabatake, Appl. Phys. Lett. **92**, 041901 (2008).
[15] K. Suekuni, M. A. Avila, K. Umeo, H. Fukuoka, S. Yamanaka, T. Nakagawa, and T. Takabatake, Phys. Rev. B **77**, 235119 (2008).
[16] G. S. Nolas, B. C. Chakoumakos, B. Mahieu, G. J. Long, and T. J. R. Weakley, Chem. Mater. **12**, 1947 (2000).
[17] R. Kröner, K. Perters, H. G. von Schnering, and R. Nesper, Z. Kristallogr. - New Cryst. Struct. **213**, 667 (1998).
[18] R. Kröner, K. Perters, H. G. von Schnering, and R. Nesper, Z. Kristallogr. - New Cryst. Struct. **213**, 671 (1998).
[19] G. S. Nolas, J. L. Cohn, J. S. Dyck, C. Uher, and J. Yang, Phys. Rev. B **65**, 165201 (2002).
[20] R. D. Shannon, Acta Crystallogr., Sect. A: Cryst. Phys., Diffr., Theor. Gen. Crystallogr. **32**, 751 (1976).
[21] M. Hayashi, K. Kishimoto, K. Kishio, K. Akai, H. Asada, and T. Koyanagi, Dalton Trans. **39**, 1113 (2010).
[22] CRYSTALSTRUCTURE3.8, Crystal Structure Analysis Package, Rigaku and MSC, 2000–2006.
[23] M. Christensen, N. Lock, J. Overgaard, and B. B. Iversen, J. Am. Chem. Soc. **128**, 15657 (2006).
[24] M. Kozina, F. Bridges, Y. Jiang, M. A. Avila, K. Suekuni, and T. Takabatake, Phys. Rev. B **80**, 212101 (2009).
[25] A. Bentien, E. Nishibori, S. Paschen, and B. B. Iversen, Phys. Rev. B **71**, 144107 (2005).
[26] J. Yang, in *Thermal Conductivity: Theory, Properties, and Applications*, edited by T. M. Tritt (Kluwer Academic, New York, 2004), p. 1.
[27] M. A. Avila, K. Suekuni, K. Umeo, H. Fukuoka, S. Yamanaka, and T. Takabatake, Phys. Rev. B **74**, 125109 (2006).
[28] I. Ishii, Y. Suetomi, T. K. Fujita, T. Tanaka, T. Onimaru, K. Suekuni, T. Takabatake, and T. Suzuki (unpublished).